MICRO THERMAL SWITCH WITH STIFFNESS ENHANCED THERMAL ISOLATION STRUCTURE

Takashiro Tsukamoto[1*], M. Esashi[2], S. Tanaka[1]
[1]Department of Nanomechanics, Tohoku University, Sendai, Japan
[2]Advanced Institute for Materials Research, Tohoku University, Sendai, Japan
*Presenting Author: t_tsuka@mems.mech.tohoku.ac.jp

Abstract: A solid contact type thermal switch requires both high contact force and high thermal isolation, but they are in tradeoff relation. This study demonstrated a novel stiffness-enhanced thermal isolation structure, which can generate high contact force but does not increase heat loss. The stiffeness of the parylene beams are multiplied by silicon stiffening beams, which apply rotational constraint to the parylene beams to reduce the equivalent length of the parylene beams. The stiffening beams are designed as it increases no additional heat loss. The silicon stiffening beams increased the stiffness of the parylene beams by a factor of 3, and the unnecessary thermal conductance was still as low as 3.7×10^{-5} W/K.

Keywords: MEMS, Thermal switch, Thermal isolation, Contact pressure, Heat loss

INTRODUCTION

Heat flow control of micro devices is important for thermal devices such as micro heat engine, micro refrigerator, micro reactor and so on. A thermal switch, which dynamically changes the contact state, i.e. thermal conductance between two objects, is commonly used for heat flow control. For example, considering a micro magnetic refrigerator using a MEMS-based thermal switch, our theoretical estimation suggests that the OFF/ON thermal resistance ratio must be at least 14 to establish the refrigerating cycle. Several types of thermal switches have been reported [1-5], but the past studies mainly focused on how to improve thermal contact conductance at ON state, e.g. using carbon nanotube (CNT) contactors [1-3,6]. Even if thermoconductive interlayers such as CNT array are used, larger contact force results in better thermal contact.

Another important factor is high thermal isolation at OFF state. We developed a parylene beam thermal isolation structure for this purpose [2]. The cross sectional area of the isolation beam should be small and the length should be large for high thermal isolation, whereas this leads to a quite low stiffness of the beam, resulting in small contact force. Therefore, high thermal contact conductance at ON state and high thermal isolation at OFF state is in tradeoff relationship. In this study, we designed and fabricated a novel stiffness-enhanced thermal isolation structure to break through this tradeoff.

THERMAL SWITCH

Structure

The structure of the thermal switch is shown in Fig. 1. Two thermal contactors which are supported by parylene beams are placed at both sides of a moving frame. The moving frame is actuated by an external actuator. The advantage of this structure is that the parylene beams thermally isolate the contactors from the other parts such as the moving frame and the external actuator, drastically decreasing the heat capacity of the contactors and thus improving thermal response. On the other hand, the parylene beams should be stiff enough to generate large contact force at ON state [1-3,6]. From this point of view, a high-aspect-ratio cross-sectional shape is preferable for the parylene beam. However, the achievable aspect ratio i.e. the obtainable stiffness of the beam is practically limited. Our proposed solution is to use silicon stiffening beams, which will be described in the next subsection. The silicon stiffening beams increase the stiffness of the parylene beams, but do not increase conductive heat loss.

Stiffness-enhanced Thermal Isolation Structure

Figure 2 explain the working principle of the silicon stiffening beams. The stiffness of a clamped cantilever with the deformation angle of the unclamped end fixed is expressed as

$$k = \frac{12\,EI}{l^3}, \tag{1}$$

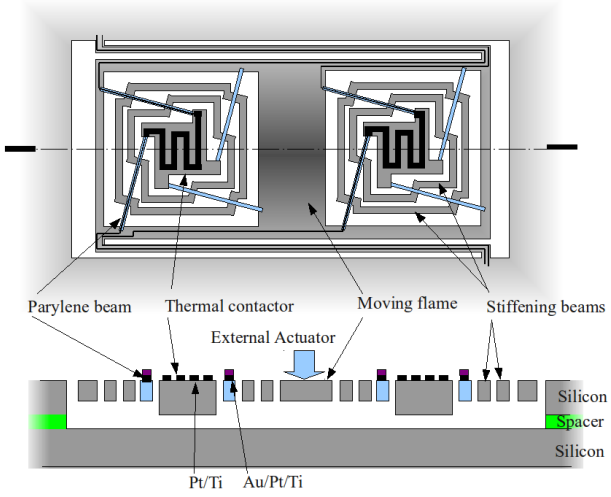

Fig. 1. Structure of the thermal switch.

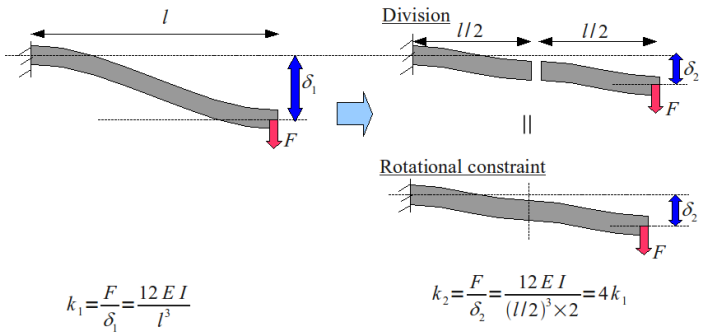

Fig. 2. Stiffening principle.

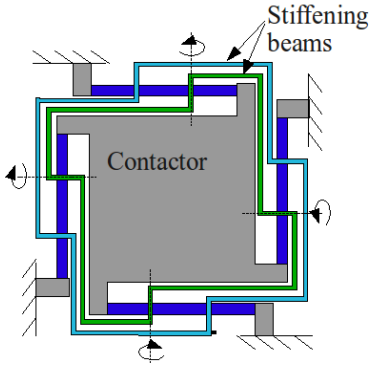

Fig. 3. Structure of the stiffening beams.

where E, I and F are the Young's module, geometric moment of inertia and length of the cantilever, respectively. According to the equation, the stiffness is inversely proportional to the 3rd power of the length. As shown in Fig. 2, if the beam is divided into two, the equivalent stiffness of these two divided beams become 4 times of the original one. The equivalent stiffness of divided beams is given by

$$k_n=\frac{12EI}{(l/n)^3}\frac{1}{n}=\frac{12EI}{l^3}n^2, \qquad (2)$$

where n is the number of division.

Practically, how to divide the beam without increase in heat loss is important. Figure 3 shows the dividing method. The stiffening beams constrain the rotation of the parylene beams, applying the same boundary condition as they are divided. The stiffening beams are made of silicon, but there is no additional heat dissipation because the strengthen beams connect between the thermally equilibrated points of the parylene beams, i.e. there is no temperature distribution within the silicon beam.

Figure 4 shows the results of steady state structural analysis using FEM. Figure 4 (a) and (b) are models without and with the stiffening beams, respectively. In Fig. 4 (b), two stiffening beams are connected to each parylene beam (i.e. n = 3). The outer sides of the parylene beams are fixed and the contactor is loaded with 5 mN (20 kPa contact pressure applied to the 500 × 500 μm^2 area). The stiffness is obtained as the applied load divided by the displacement of the contactor. Comparing the structures shown in Fig. 4 (a) and (b), the stiffness is increased with a factor of 3 (k_3/k = 3). This is smaller than the theoretical value, $k_3/k = 3^3 = 9$, because the stiffening beam is not completely rigid and is twisted.

Figure 5 shows the results of thermal analysis. The temperature is fixed to be 300 K at the outside of the parylene beams. The thermal conductance is obtained as the applied heat input divided by the temperature difference between the contactor and the ambient (= 300 K). From Fig. 5 (a) and (b), the thermal conductance without and with stiffening beams are obtained as 1.3 × 10^{-5} W/K and 1.6 × 10^{-5} W/K,

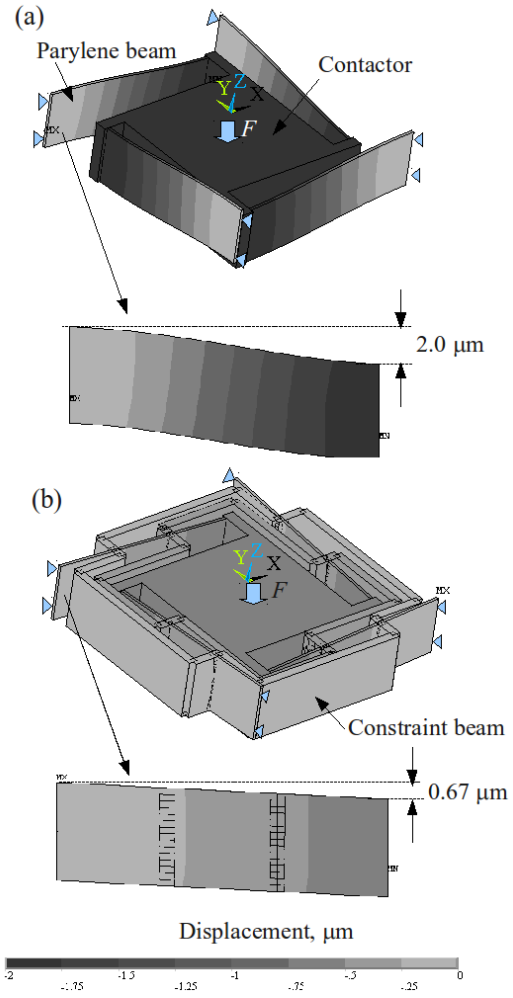

Fig. 4. FEM simulation of stiffness (a) without and (b) with stiffening beams.

respectively. The thermal conductance increase ca. 20 %, whereas the stiffness increase ca. 200 %.

Fabrication Process

Figure 6 shows the fabrication procedure. First, silicon is etched by DRIE to form high aspect ratio trenches for parylene beam mold [7]. Parylene is deposited to fill the trench, and then the surface is ground and polished to remove unwanted parylene. A Au/Pt/Ti thin film is deposited and patterned by lift-off method. The Au layer on the contactor is etched to form a Pt thin film resistor. Backside silicon is etched

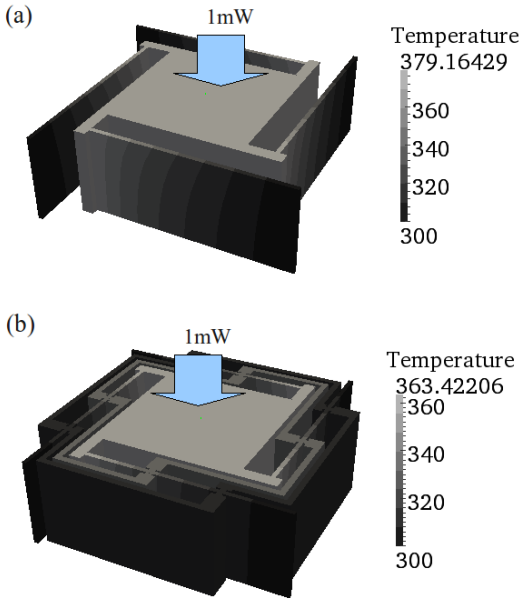

Fig. 5. FEM thermal simulation of (a) without and (b) with stiffening beams.

to define the shape of the contactor. Finally, the silicon mold is etched to release parylene beams. Figure 7 is the photograph of the contactor and the beams.

MEASUREMENT PROCEDURE

Thermal conductance is measured by thermal response. The temperature response of the contactor is estimated by a theoretical model as shown in Fig. 8. It consists of two heat capacitors (C_1: Contactor, C_2: External frame) and two heat resistances (R_1: Parylene beams, R_2: Thermal dissipation to ambient). The thermal conductance is obtained by fitting the theoretical response to the experimental results. The step response of the temperature T is given by

$$\Delta T = \frac{Z}{X}\left(1-e^{-Xt}\right)+\frac{W}{Y}\left(1-e^{-Yt}\right), \qquad (3)$$

where X, Y, Z and W are defined by the following equations using $\tau_1 = (R_1C_1)^{-1}$, $\tau_2 = (R_1C_2)^{-1}$ and $\tau_3 = (R_2C_2)^{-1}$:

$$X = \frac{\left(\frac{1}{\tau_1}+\frac{1}{\tau_{12}}+\frac{1}{\tau_2}\right)-\sqrt{\left(\frac{1}{\tau_1}+\frac{1}{\tau_{12}}+\frac{1}{\tau_2}\right)^2-\frac{4}{\tau_1\tau_2}}}{2}.$$

$$Y = \frac{\left(\frac{1}{\tau_1}+\frac{1}{\tau_{12}}+\frac{1}{\tau_2}\right)+\sqrt{\left(\frac{1}{\tau_1}+\frac{1}{\tau_{12}}+\frac{1}{\tau_2}\right)^1-\frac{4}{\tau_1\tau_2}}}{2}.$$

$$Z = \frac{q}{C_1}\left(\frac{1}{2}+\frac{-\frac{1}{\tau_2}+\frac{1}{\tau_{12}}+\frac{1}{\tau_2}}{2\sqrt{\left(\frac{1}{\tau_1}+\frac{1}{\tau_{12}}+\frac{1}{\tau}\right)^2-\frac{4}{\tau_1\tau_2}}}\right).$$

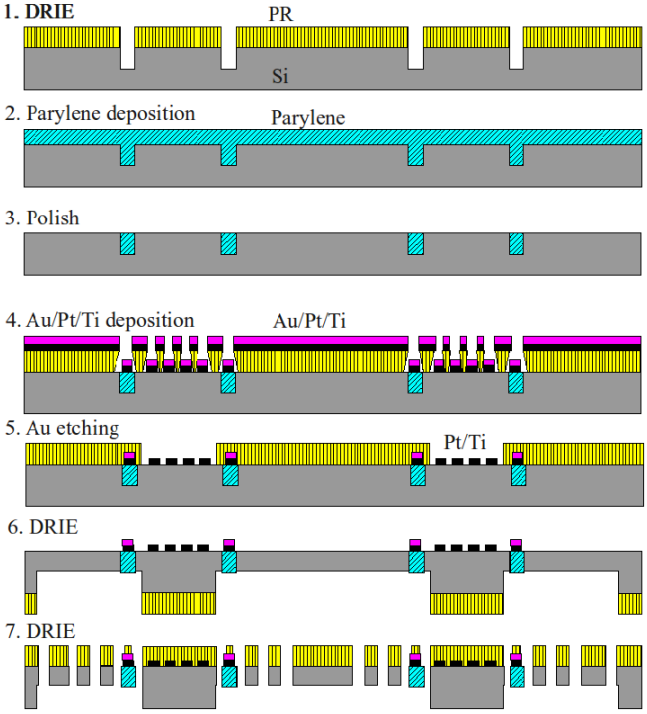

Fig. 6. Fabrication process.

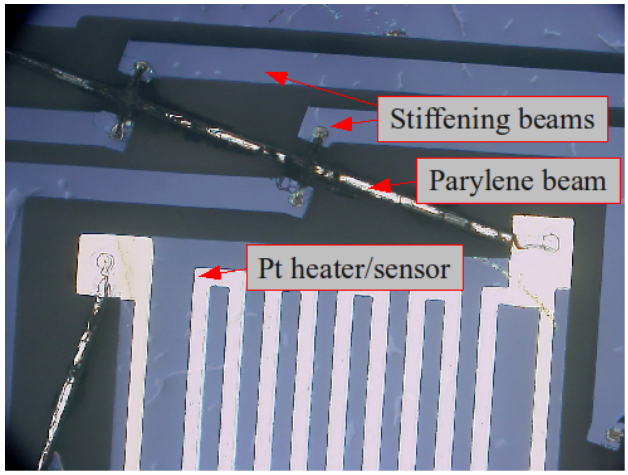

Fig. 7. Thermal contactor with constrain beams.

$$W = \frac{q}{C_1}\left(\frac{1}{2}-\frac{-\frac{1}{\tau_1}+\frac{1}{\tau_{12}}+\frac{1}{\tau_2}}{2\sqrt{\left(\frac{1}{\tau_1}+\frac{1}{\tau_{12}}+\frac{1}{\tau_2}\right)^2-\frac{4}{\tau_1\tau_2}}}\right).$$

The fabricated device is placed in a vacuum chamber to minimize unnecessary heat loss. The thin film Pt resistor fabricated on the contactor is used as both heater and temperature sensor.

EXPERIMENTAL RESULT

Figure 8 shows the measured temperature response, which was obtained under the condition that the input heat rate was constant. The ambient pressure was ca. 1 Pa. The measured temperature change is preprocessed according to

$$-\ln\left(1-\frac{\Delta T}{\Delta T_\infty}\right)=Xt-\ln\left(A+(1-A)e^{-|Y-X|t}\right), \quad (4)$$

which is obtained from Eq. (3). In Eq. (4), ΔT and ΔT_∞ are measured temperature change and saturated temperature change, respectively, and A is defined by

$$A=\frac{1}{1+\frac{X}{Y}\frac{W}{Z}}.$$

Fitting Eq. (4) to the experimental result gives thermal conductance, $1/R_1$. To make the fitting easy, Eq. (4) is approximated into two asymptotic lines in regions of $t \approx 0$ and $t \gg \frac{1}{1/\tau_1+1/\tau_{12}+1/\tau_2}$. Figure 8 includes these two asymptotic lines. The obtained thermal conductance is 3.7×10^{-5} W/K, which is roughly same as the estimated value obtained from FEM simulation (1.6×10^{-5} W/K). The difference is considered as uncertainty of thermal property of the thin film materials and the error of simplified heat loss models of radiation and gas molecule conduction.

Our previous study found that the thermal contact resistance depends on the contact pressure to the power of –0.5 [3]. Then the contactor with the stiffening beams can increase the thermal conductance by 70 % with a constant actuation stroke, whereas heat loss increase only 20 %. The thermal contact resistance of the CNT contactor is ca. 8.3×10^{-4} W/K, when the contact pressure is 20 kPa [3]. In this condition, this thermal switch can achieve an OFF/ON thermal resistance ratio as high as 23.

CONCLUSION

We designed and fabricated a microstructure with high thermal isolation and high stiffness for a thermal switch. Thermal isolation is realized by high-aspect-ratio parylene beams fabricated by silicon lost molding. The stiffness of the parylene beams are multiplied by silicon stiffening beams, which constrain the deformation angle of the parylene beams but do not increase heat loss. The effect of this structure was confirmed by both simulation and experiment. The silicon stiffening beams increased the stiffness of parylene beams by a factor of 3, but did not add significant heat loss.

ACKNOWLEDGEMENT

This study was partly supported by the Ministry of Education, Science, Sports and Culture, Grant-in-Aid for Exploratory Research, No. 20651036, 2008. T. Tsukamoto was supported by Research Fellowship for Young Scientist, Japan Society for the Promotion of Science (JSPS).

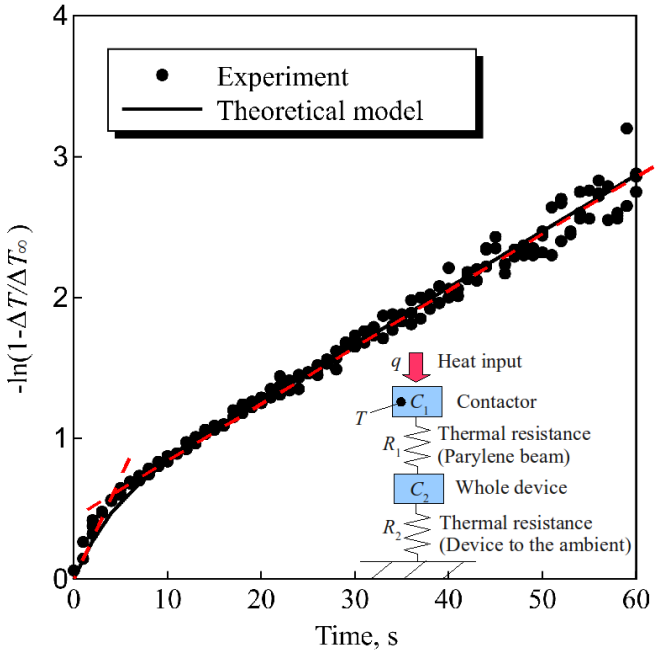

Fig. 8. Step response of Temperature.

REFERENCES

[1] Cho J, Richards C, Bahr D, Jiao J, Richards R 2008 Evaluation of contacts for a MEMS thermal switch *J. Micromech. Microeng.* **18** 105012

[2] Tsukamoto T, Esashi M, Tanaka S 2009 LOW CONTACT RESISTANCE MICRO THERMAL SWITCH WITH CARBON-NANOTUBE-ENHANCED CONTACTOR in *Proc. Transducers 2009 (Denver, USA, 21-25 June 2009)* 1489-1492

[3] Tsukamoto T, Esashi M, Tanaka S 2010 Carbon-Nanotube-Enhanced Thermal Contactor in Low Contact Pressure Region *Jpn. J. Appl. Phys.* **49** 070210

[4] Gong J, Cha G, Ju Y S, Kim C-J 2008 THERMAL SWITCHES BASED ON COPLANAR EWOD FOR SATELLITE THERMAL CONTROL in *Proc. MEMS 2008 (Tucson, USA, 13-17 January.2008)* 848-851

[5] Kim H-S, Liao H-H, Song H O, Kenny T W 2008 VARIABLE THERMAL RESISTORS (VTR) FOR THERMAL MANAGEMENT OF CHIP SCALE ATOMIC CLOCKS (CSAC) *in Proc. MEMS 2008 (Tucson, USA, 13-17 January 2008)* 852-855

[6] Xu J, Fisher T S 2006 Enhancement of thermal interface materials with carbon nanotube arrays *Intl. J. Heat and Mass Transfer* **49** 1658−1666

[7] Suzuki Y, Tai Y-C 2006 Micromachined High-Aspect-Ratio Parylene Spring and Its Application to Low-Frequency Accelerometers *J. Microelectromech. Syst*. **15** 1364−1370